Journal of Radiation Research and Applied Sciences

ISSN: (Print) (Online) Journal homepage: https://www.tandfonline.com/loi/trra20

Transcriptional modulations induced by proton irradiation in mice skin in function of adsorbed dose and distance

Valerio Licursi, Wei Wang, Elena Di Nisio, Francesco P. Cammarata, Rosaria Acquaviva, Giorgio Russo, Lorenzo Manti, Mariangela Cestelli Guidi, Emiliano Fratini, Gihan Kamel, Roberto Amendola, Pietro Pisciotta & Rodolfo Negri

To cite this article: Valerio Licursi, Wei Wang, Elena Di Nisio, Francesco P. Cammarata, Rosaria Acquaviva, Giorgio Russo, Lorenzo Manti, Mariangela Cestelli Guidi, Emiliano Fratini, Gihan Kamel, Roberto Amendola, Pietro Pisciotta & Rodolfo Negri (2021) Transcriptional modulations induced by proton irradiation in mice skin in function of adsorbed dose and distance, Journal of Radiation Research and Applied Sciences, 14:1, 260-270, DOI: 10.1080/16878507.2021.1949675

To link to this article: https://doi.org/10.1080/16878507.2021.1949675

JOURNAL OF RADIATION RESEARCH AND APPLIED SCIENCES
2021, VOL. 14, NO. 1, 260–270
https://doi.org/10.1080/16878507.2021.1949675

Transcriptional modulations induced by proton irradiation in mice skin in function of adsorbed dose and distance

Valerio Licursi[a], Wei Wang[a], Elena Di Nisio[a], Francesco P. Cammarata[b,c], Rosaria Acquaviva[c,d], Giorgio Russo[b,c], Lorenzo Manti[e,l], Mariangela Cestelli Guidi[f], Emiliano Fratini[g], Gihan Kamel[h,i], Roberto Amendola[j], Pietro Pisciotta[b,c,k] and Rodolfo Negri[a]

[a]Department of Biology and Biotechnologies C. Darwin, Sapienza University of Rome, Rome, Italy; [b]Institute of Molecular Bioimaging and Physiology (IBFM-CNR) , CNR, Cefalù (PA), Italy; [c]Laboratori Nazionali del Sud, INFN, Catania, Italy; [d]Department of Drug and Health Science, Biochemistry section, University of Catania, Catania, Italy; [e]Department of Physics "E. Pancini" University of Naples Federico II, University of Naples Federico II, Naples, Italy; [f]Laboratori Nazionali di Frascati, INFN, Frascati, Italy; [g]Department of Science, University of Rome "Roma Tre", Rome, Italy; [h]SESAME (Synchrotron - Light for Experimental Science and Applications in the Middle East), Allan, Jordan; [i]Department of Physics, Faculty of Science, Helwan University, Cairo, Egypt; [j]SSPT-TECS-SAM, CR Casaccia, ENEA, SSPT-TECS-SAM, CR Casaccia, Rome, Italy; [k]Department of Radiotherapy, University of Groningen, University Medical Center Groningen, The Netherlands; [l]Section of Naples, INFN, Naples, Italy

ABSTRACT

Hadron therapy by proton beams represents an advanced anti-cancer strategy due to its highly localized dose deposition allowing a greater sparing of normal tissue and/or organs at risk compared to photon/electron radiotherapy. However, it is not clear to what extent non-targeted effects such as transcriptional modulations produced along the beamline may diffuse and impact the surrounding tissue. In this work, we analyze the transcriptome of proton-irradiated mouse skin and choose two biomarker genes to trace their modulation at different distances from the beam's target and at different doses and times from irradiation to understand to what extent and how far it may propagate, using RNA-Seq and quantitative RT-PCR. In parallel, assessment of lipids alteration is performed by FTIR spectroscopy as a measure of tissue damage. Despite the observed high individual variability of expression, we can show evidence of transcriptional modulation of two biomarker genes at considerable distance from the beam's target where a simulation system predicts a significantly lower adsorbed dose. The results are compatible with a model involving diffusion of transcripts or regulatory molecules from high dose irradiated cells to distant tissue's portions adsorbing a much lower fraction of radiation.

ARTICLE HISTORY
Received 6 December 2020
Accepted 24 June 2021

KEYWORDS
Proton irradiation; hadrontherapy; transcriptome modulation; mouse skin; spectroscopy FTIR microspectroscopy

1. Introduction

A deep understanding of biological consequences of ionizing radiation exposure requires a better knowledge of many aspects of the cellular and tissue response to the radiation insult. Previous literature suggests the existence of complex intracellular and inter-cellular damage signaling pathways in eukaryotic cells that regulate the response to radiation, modulating cell-cycle progression, stimulating DNA repair, and eventually triggering programmed cell death (Santivasi & Xia, 2014; Weichselbaum et al., 1991). In mammalian cells, a major component of this biological response is mediated by gene transcription modulation (Amundson, 2008; Chiani et al., 2009; Woloschak & Chang-Liu, 1990). This transcriptional response can considerably change on a quantitative and qualitative point of view, in function of cell type, dose and quality of radiation (Bufalieri et al., 2012; Giusti et al., 2014). Moreover, tissue response to irradiation is very complex and cannot be recapitulated by studies on isolated cell lines in active proliferation, involving completely different signaling pathways (Bufalieri et al., 2012; Fratini et al., 2011; Hamada et al., 2016; Licursi et al., 2017). Several studies suggested that the radiation response is not limited to the targeted cells but can propagate to surrounding cells and tissues, a phenomenon known as bystander effects (Brooks et al., 1974; Marín et al., 2015; Mothersill & Seymour, 2006) and even to untargeted organs (abscopal effects, (Mole, 1953; Yilmaz et al., 2019). Despite many studies suggested plausible explanations and a long list of possible effector molecules for this propagation, detailed mechanisms are still elusive, at least for what has been observed on tissues *in vivo*. Radiotherapy still represents one of the best strategies to defeat tumors. While the cellular damage caused by low LET radiation is sparse and partially dependent on cellular redox metabolism and proliferation, high LET radiation produces localized complex lesions along the particles' tracks which result more difficult to be repaired.

CONTACT Mariangela Cestelli Guidi mariangela.cestelliguidi@lnf.infn.it INFN Laboratori Nazionali Di Frascati, Via Enrico Fermi 54, Frascati 00044, Italy

Supplemental data for this article can be accessed here.

(Cohen & Awschalom, 1982; Durante, 2014; Xue et al., 2009). Off-target effects are a crucial issue in radiotherapy: although irradiation protocols are becoming very accurate, the perspective of unwanted harmful effects in tissues adjacent to the tumor is still worrisome. Radiation-induced subcutaneous fibrosis (RIF) is a common long-term effect following conventional radiotherapy whose painful symptoms limit therapeutic doses (Westbury & Yarnold, 2012). Particle therapy as carried out by proton and carbon ion beams indeed represents an advanced anti-cancer strategy due to its highly localized dose deposition on target tissue and lower 'dose bath' on normal tissue (Durante & Flanz, 2019) but at the moment it is not clear to what extent may the modifications induced by irradiation diffuse to surrounding tissue. In recent years, the appealing properties of the high-energy protons made the interest in their therapeutic use constantly growing (Tommasino & Durante, 2015). Indeed, proton irradiation may reduce the total radiation dose to normal tissue by approximately 60% (Miralbell et al., 2002). Clinical proton RBE is assumed to be 1.1, however, it remains to be established the impact of increasing LET toward the distal end of the Spread-out Bragg Peak (SOBP), which may result in a higher-than expected damage, as well as the biological consequences of the neutrons produced along the beamline. In fact, cellular response to protons may differ significantly from what can be predicted solely by physical properties (Girdhani et al., 2012; Tian et al., 2011). For example, it is not known how bystander signaling may extend the toxic and functional effects to the proximal unirradiated tissue (Vitti & Parsons, 2019). At least for RIF, a role of transcription modulation induced by particles irradiation has been shown (Nielsen et al., 2017) and differential gene expression has been previously used to predict sensitivity or resistance to RIF in breast cancer patients (Alsner et al., 2007). In this study, we focus on the diffusion of transcription modulation. We trace the modulation of two biomarker genes by proton irradiation of mouse skin at different distances from the beam's target and at different doses and times from irradiation to understand to what extent and how far it may propagate. The results suggest that the diffusion distance of the modulation depends on both the dose administered and the particular modulated gene, being driven by both adsorbed radiation and diffusion of regulatory molecules from cell to cell.

2. Materials and methods

2.1. Irradiation

Experimental design

Experiments were performed on 6-week-old C57BL/6 male mice (Charles River Laboratory), weighing 27 ± 3 gr. Animals were housed in IVC-cages at constant temperature (23–25°C) under a 12/12 h light/dark cycle with ad libitum access to food and water. A total number of 30 animals was used in this study. Mice were randomly assigned to Sham-control group (n = 6) and treated group (n = 24). Before each irradiation, the mice were anesthetized with Zoletil (tiletamine) 40 mg/kg and Sedastart (medetomidine) 50 µg/kg. All experiments were performed in accordance with the European Communities Council directive and Italian regulations (EEC Council 2010/63/EU and Italian D.Lgs. 26/2014) and all efforts were made to replace, reduce and refine the use of laboratory animals.

2.2. CATANA experimental room and dose delivery system

The experimental measurements were performed at the CATANA proton therapy facility (beam of 62 MeV/A of energy) for the therapeutic treatment of choroidal or iris melanoma, eye melanoma tumors (INFN-LNS, Catania, Italy). Starting from 2016, CATANA facility allows animal irradiation, in collaboration with University of Catania, taking the advantage of a dedicated holding system in-house designed to perform high precision and reproducible small animal irradiation (Givehchi et al., 2011; Russo et al., 2017). The beam goes out in the air and flies for 3 m traversing through elements modifying its energy and the shape before hitting the target (scattering foils spreading the beam laterally; collimators defining beam profile and target shape; range shifter and modulator wheel modifying the particle range and the SOBP dimension). The lateral homogeneity was the same used during patient treatment and the dose variation is less than 2% at irradiation position. All animals were irradiated using a degraded SOBP realized using a PMMA modulator wheel with 14.8 mm of plateau and a practical range of 30.2 mm; at the irradiation time a range shifter was placed to position the skin. The dose accuracy is assumed to be about 3%. The field size was shaped using a brass in-house-made collimator that centered into the target part of mice. The dosimetry was performed by a Markus ionization chamber (PTW Freiburg GmbH, Germany) with gafchromic EBT3 films (ISP Corp., New York, USA). At each irradiation, the gafchromic EBT3 film was placed before the target to control the beam flatness and the released dose. Like for radiotherapy, the dose delivered at the experimental proton beam line was monitored by a transmission ionization chamber placed along the beam line that automatically switches off the beam when the requested number of monitor units (MU) are reached. A constant dose rate of 5 Gy/min was set for all the irradiations. All animal irradiations were performed at the same hour of the day to

guarantee no response difference related to circadian rhythm of the mice. Irradiation was delivered at the two doses of 1 Gy and 0.1 Gy, and mice were euthanized after 6 h and 24 h. Both doses are not considered lethal and do not cause pain.

2.3. Prediction of adsorbed dose

Currently, Monte Carlo (MC) methods are largely and routinely used in clinical application since they produce accurate and efficient prediction on dose distribution. MC simulations become an essential tool when small animals are irradiated and when the dimension of targets are less than few centimeters. In this study, a GEANT4-based application (Allison et al., 2006) has been employed to evaluate the dose distributions in small animals irradiated at the CATANA experimental room. At this purpose, this application gives the chance to implement the target through its DICOM microCT images (Pisciotta et al., 2018; Russo et al., 2017) permitting to investigate the interaction of the proton beam released at CATANA experimental room with the real small animals anatomy. In detail, the GEANT4 application permits to simulate entirely the CATANA proton beamline and defines voxel-by-voxel the composition of the target using its DICOM micro-CT (Pisciotta et al., 2018; Russo et al., 2017). The micro-CT datasets were acquired using a preclinical micro-PET/CT (Albira Si, Bruker) available at CAPiR (Center for Advanced Preclinical in vivo Research), University of Catania, Italy. The datasets were acquired using 600 views in high resolution configuration, an X-Ray energy of 45 kVp, a current of 400 μA and the dimension of each CT-voxel was equal to 125 x 125 × 125 μm^3. The hadronic and the electromagnetic processes involved in the beam-tissue interaction were simulated using *QGSP_BIC* and *G4EmStandardPhysics option4 physics lists*. The first one is recommended when proton energies are below 200 MeV, and it includes the Binary cascade model. The latter is a *Physics Constructor* class designed for any applications requiring higher accuracy of electrons, hadrons, and ion tracking. It uses the most accurate standard and low-energy models and a set of EM processes with accurate simulations of neutral and charged particle transport. Both models have been widely validated for proton incident beams in the energy range used in this study (Hall et al., 2016).

2.4. RNA-Sequencing

Total RNA was isolated from frozen mouse skin samples using the miRNeasy Mini Kit (Qiagen). RNA quality control and measures were performed with a NanoDrop 1000 spectrophotometer (Thermo Scientific). IGA Technology Services (Udine, Italy) created the RNA-Seq libraries using the Illumina TruSeq RNA Sample Preparation Kit V2 (Illumina, San Diego, USA) and sequenced them as specified by the manufacturer's instructions using an Illumina HiSeq2000.

For each library have been generated about 40 million of single end reads of 75 base pairs. Reads quality was checked using FastQC (version 0.11.2, Babraham Institute Cambridge, UK) tool, then reads were mapped to the mouse Ensembl GRCm38 transcriptome index (release 84) using kallisto (version 0.43.0) (Bray et al., 2016). The following flags were used for kallisto: -single -l 200 -s 20. Gene-level normalization and differential gene expression analysis were performed using Bioconductor (Gentleman et al., 2004) R (version 3.2.2) (R Core Team, 2015) package DESeq2 (version 1.16) (Love et al., 2014). Principal component analysis of the sample gene profiles was performed with prcomp function and plotted using ggplot2 package in R. In order to understand biological meaning of the differentially expressed genes the resulting filtered (adjusted p-value < 0.1) genes were clustered by functional annotation using DAVID web tool (Dennis et al., 2003; Huang et al., 2009).

2.5. Real-time RT-PCR

For each RNA sample, 0.5 μg of total RNA was reverse-transcribed using the QuantiTect Reverse Transcription Kit (Qiagen) and amplified with a 7500 Fast Real-Time PCR System (Applied Biosystems), using the SensiFAST™ SYBR® LoROX Kit (Bioline) and MicroAmp® Optical 96-Well Reaction Plates (Applied Biosystems), as specified by the manufacturer. Relative abundance of transcripts was calculated with the 2^(-ΔΔCt) method, using TAF14 as a reference gene. The sequences of the primers used for real-time RT-PCR assays are available upon request.

2.6. FT-IR spectroscopy analysis of lipid alteration

FT-IR spectra were collected at the SESAME IR Synchrotron radiation beamline (Kamel et al., 2017) and at the INFN Dafne-Light IR beamline (Cestelli Guidi et al., 2005). Samples from irradiated mice were preserved at −80°C and then sectioned in a cryo-microtome. The 6 micron thickness tissue slices were deposited on ZnSe infrared transparent windows and fixed in a solution containing 1% of paraformaldehyde. Absorption spectra were collected in transmission mode at 4 cm^{-1} resolution and 256 scans, using an infrared microscope coupled to a FT-IR spectrometer with 15X objective. Focal Plane Array maps were also collected with a globar source for a preliminary screening to define the region of analysis

(Supplementary file, Fig. 8). For quantitative data analysis, the same 20 μm area (i.e. close to the bulb hair) was considered for all the samples. The four skin sampling positions corresponded to beam entrance (muscle of the right hind leg) or 15, 26, and 40 mm distance (toward right flank), respectively dubbed as E1, E2, E3, and E4, (where E1 is the beam entrance). Large tissue maps (500x600 microns) were collected using a motorized micrometric stage and 20 μm step. Oxidative stress is one of the main factors determining radiation damage in biomolecules in living tissues. Among the various cellular components, the double layer of phospholipidic membranes is extremely vulnerable to attacks by oxidizing species due to the presence of a large number of unsaturated bonds, which are more reactive (Abdelrazzak & El-Bahy, 2018). Following exposure to ionizing radiation, the phospholipidic cell membrane can be deformed with the direct consequence of a loss of integrity and functionality. The evaluation of specific lipid absorption bands intensity can be therefore considered an alternative method for the determination of the oxidative stress and the induced disorder of the hydrocarbon lipid chains. In addition to phospholipid membranes, proteins are also targets for radiation-induced oxidative stress (Gianoncelli et al., 2015; Panganiban et al., 2013). Highly reactive oxygen species interact with proteins, mainly with the hydrogen bond in the protein backbone, causing a variation in their secondary structure which, in extreme cases, leads to denaturation and loss of functionality (Boyd-Kimball et al., 2005). The infrared absorption spectra of sham-irradiated samples, 0.1 Gy and 1 Gy are shown in Suppl. Fig. 9. To give an estimate of the extent of the radiative damage at the molecular level, we focused first on the structure of the lipid membranes. In particular, the asymmetric stretching of methyl and methylene groups ($_{as}CH_3$, $_{as}CH_2$) and the ester carbonyl band (C = O) have been divided by the area under the entire lipid stretching region centered at 2800–3000 cm^{-1} to evaluate, respectively, the length of the hydrocarbon chain of the membrane phospholipids and lipid peroxidation. The lipid bands have been also normalized for the total amide band to evaluate the relationship between lipids and proteins in the tissues, which has been observed to be correlated to high LET radiation damage (Cestelli Guidi et al., 2012). For a complete assignment of the IR absorption bands, see SM Table 4. Calculating the ratios between the different functional groups compensate also for any artifacts caused by variations in the thickness of the tissue sections.

3. Results

3.1. Transcriptional response of mouse skin to proton-irradiation

In order to analyze the transcriptional response of mouse skin to proton irradiation, 12 mice were irradiated with a 1 Gy proton dose. At six hours after exposure, 6 mice were lethally anesthetized and skin dissection was performed at the proton beam entrance target site (muscle of the right hind leg, E1) or at 15 mm distance from it (E2, right flank). Total RNA was purified from the irradiated mice samples or from control samples (6 sham-irradiated mice, fixing E1 sampling position arbitrarily but in the identical body position). RNA-Seq was performed from all samples and compared. Principal Component Analysis (PCA) showed a high heterogeneity of transcriptome profiles in all groups, likely due to high basal expression variability, as shown by the spreading of control samples in both dimensions. In particular, one of the 6 E1 irradiated samples profile was highly different from all the others and therefore it was left out from further analyses. Partial clustering was observed for the other five E1 samples as compared with untreated controls and E2 samples (Suppl. Fig. 1). Next, we analyzed those genes that were differentially expressed among the three groups. We observed statistically significant (FDR<0.1) modulations only for the E1 group. Data reported on SM Table 1 show that following 1 Gy irradiation, 825 genes were repressed at least by a two-fold factor whereas 85 genes were upregulated at least two-fold (SM Table 1 and Suppl. Fig. 2). Most of these genes were similarly modulated in the E2 group, even though not significantly, due to high variability (not shown). Gene ontology analysis on the 85 induced genes showed 'Immunity and Immune system' and 'Disulfide bond and glycoprotein' as the most over-represented GO terms clusters (Suppl. Fig. 3). These terms clusters were both highly enriched in the list of genes modulated by neutron irradiation in mice skin (Fratini et al., 2011, see supplementary materials). As regards the repressed genes list, we found enrichment for 'mitochondrial and respiration functions' together with 'myofibril assembly and actin filament organization' which was also enriched in the neutron modulated genes list (Suppl. Fig. 4–5 and Fratini et al., 2011) and again 'Disulfide bond and glycoprotein.' The significantly modulated genes in common between mouse skin neutron and proton irradiation are 56 (SM Table 2 and 3), which represents a tissue response to particle irradiation. The similarity is also supported by the observed modulation (although not statistically significant) by proton irradiation of a group of 17 keratin and keratin-associated genes which were similarly modulated by neutrons (not shown). As it was evident from neutron irradiation, the transcriptional response of skin to proton irradiation is very different from what it is typically observed with cell lines actively replicating in culture. Few damage checkpoint-controlled genes appear modulated and to a very limited extent (i.e. CDKN1A, see Suppl. Fig. 6), while unusual coordinated responses are observed. The most striking one is

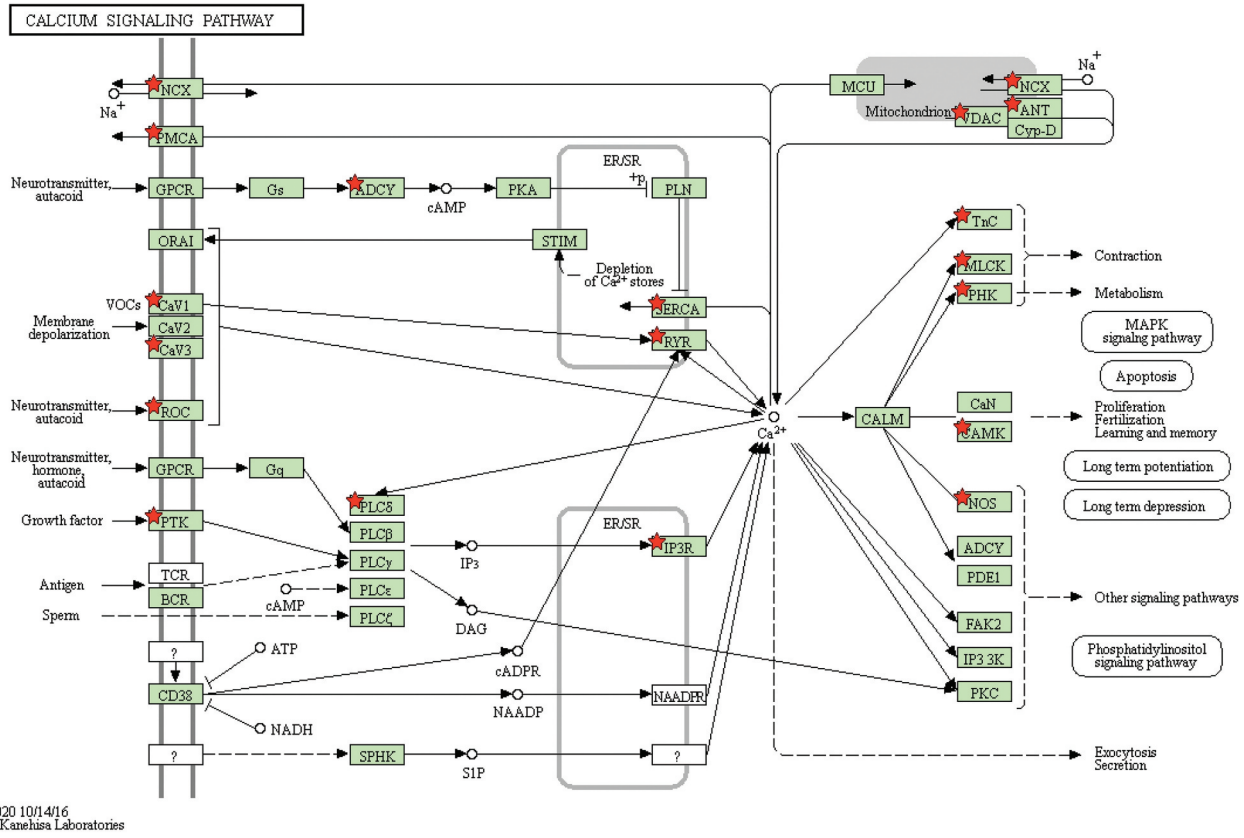

Figure 1. Genes belonging to Keggs Calcium Signaling Pathway which are significantly repressed in the E1 group. Repressed genes are indicated by a red star.

represented by the observed coordinated negative modulation of the calcium signaling pathway (Figure 1). 31 genes with an established role in this pathway are down-regulated in the E1 group, an enrichment with high statistical significance ($P < 10^{-5}$). Metabolic pathways alterations are also observed, as in the case of the negative modulation of glucagon pathway (Suppl. Fig. 7).

3.2. Transcriptional modulation in function of dose and distance from the target and time

Once we identified a list of proton-modulated genes, we planned to test the modulation of a couple of them as a function of dose and distance from the beam's target in individual mice in order to estimate the capacity of propagate. Samples of skin were taken in mice irradiated with 0.1 Gy (dose X) or 1 Gy (dose Y) at the target (E1), or at 15 mm (E2), 26 mm (E3) or 40 mm (E4) distance, at 6 or 24 hours from irradiation. A Monte Carlo simulation code was used to predict the doses delivered at the E2, E3, and E4 distances from the target. Table 1 shows the predicted doses as a function of the distance from the beam's target for the 0.1 and the 1 Gy dose, respectively. We selected one upregulated (TNFSF18) and one downregulated (CACNG1) gene. They were selected based on the following criteria:

Table 1. Predicted doses at the indicated distance from the proton beam according to Montecarlo simulation (see Materials and Methods).

Average dose (Group Y)	Distance from target	Gy
Delivered	E1 = 0 mm	1
Predicted	E2 = 15 mm	0.3791
Predicted	E3 = 26 mm	0.044
Predicted	E4 = 40 mm	0.0021

Average dose (Group X)	Distance from target	Gy
Delivered	E1 = 0 mm	0.1
Predicted	E2 = 15 mm	0.03791
Predicted	E3 = 26 mm	0.0044
Predicted	E4 = 40 mm	0.00021

(a) both of them were well expressed in skin;
(b) Both of them were robustly modulated by 1 Gy of protons at E1 distance (see SM Table 1);
(c) They showed a low rank (66th and 16th percentile rank, respectively) in the 'DE prior' list that reports the tendency of mammalian genes to be not specifically modulated in response to cellular homeostasis perturbations (Crow et al., 2019);
(d) They were obviously involved in tissutal response to radiation: TNFSF18 is emerging as a key gene in cancer resistance to radiation (see discussion), while CACNG1 is involved in calcium signaling, which is emerging as a relevant factor in regulating radiation- induced apoptosis.

Modulation was tested by real time RT-PCR, using the gene TAF14, which does not considerably change in the RNA-Seq experiment, as endogenous calibrator. Fig. 2 shows modulation of TNFSF18 in individual mice as a function of dose, distance, and time from irradiation. (Figure 2) A group of four sham-irradiated mice was used for comparison. It is clear that at low dose the gene appears induced at E1 both at 6 h and at 24 h, while samples at E4 did not show this significant up-regulation, showing expression levels similar to sham-irradiated samples. At the higher dose of 1 Gy, it shows up-regulation in E1 and E2, both at 6 and 24 hs and again E4 is significantly down-regulated in comparison to E1. CACNG1 shows significant down-regulation at E1, E2 at low dose, 6 hours and at E1, E2, and E3 at 24 h. At higher dose, modulation is significant even at E4 (Figure 3). From these data, we can conclude that both genes show a dose- and distance-

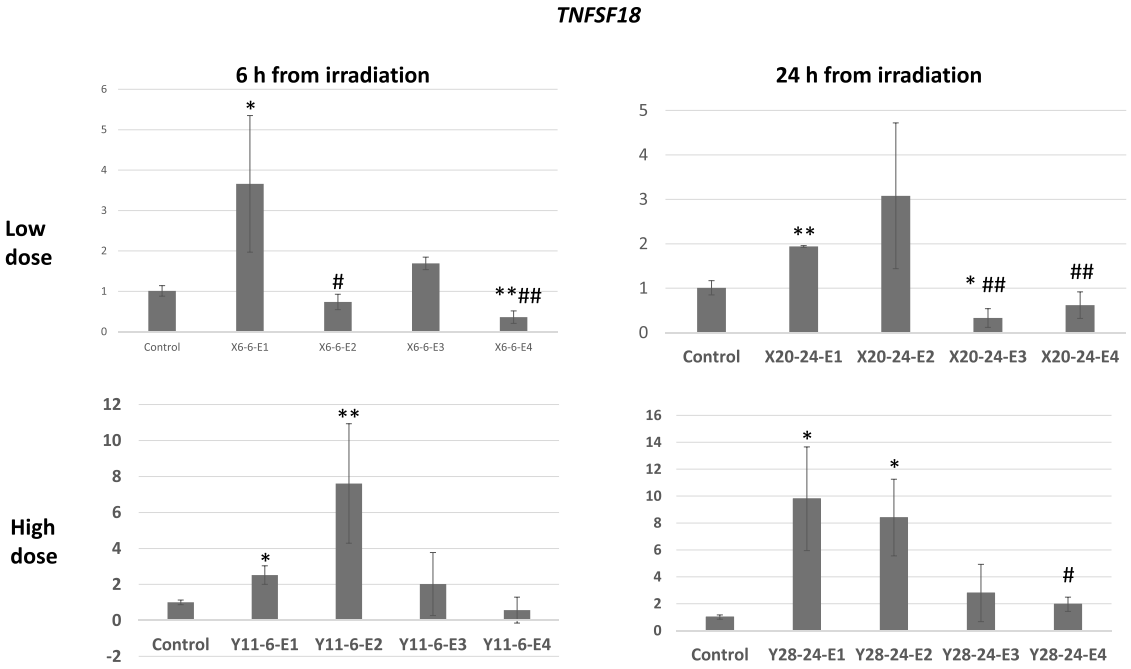

Figure 2. Expression of TNFSNF18 in samples of individual mice taken at the indicated distance (E1-E4), dose (X=0.1 Gy, Y=1 Gy) and time from irradiation. Data are normalized to TAF14 values, used as endogenous calibrator and represents the average value of three real time RT-PCR experiments. Standard deviation is indicated. The average values of four sham-irradiated control mice is reported from comparison. P-values of statistical significance were calculated by Students T-test: *< 0.05 compared to control population; **< 0.01 compared to control population; # < 0.05 compared to E1 distance; ## < 0.01 compared to E1 distance.

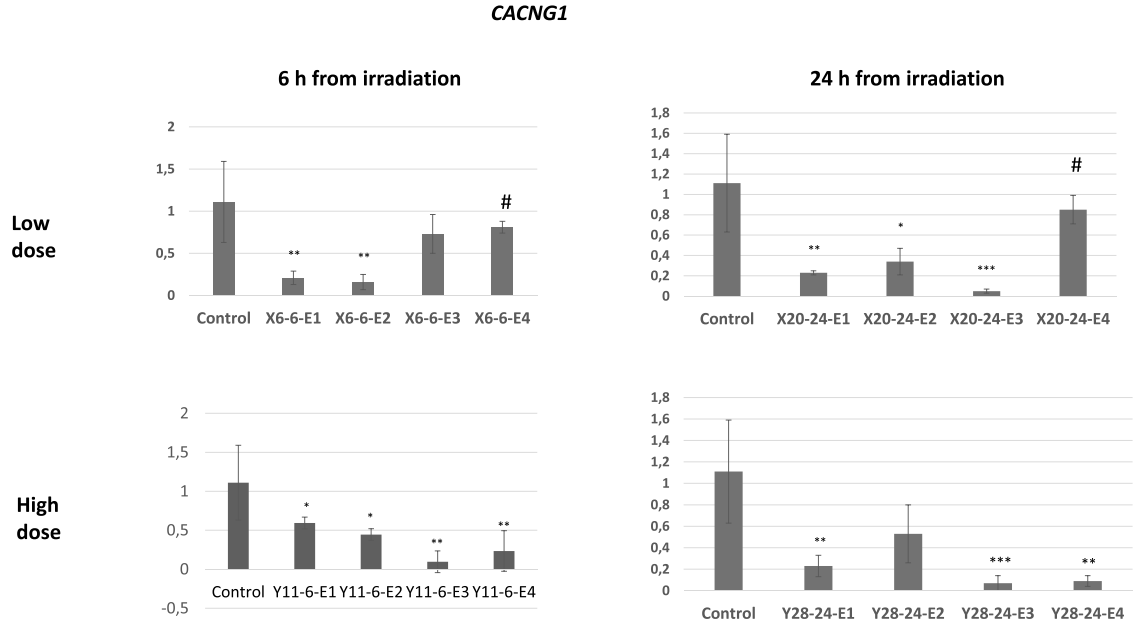

Figure 3. Expression of CACNG1 in samples from populations of 4 individual mice taken at the indicated distance (E1-E4), dose (X=0.1 Gy, Y=1 Gy) and time from irradiation. Data are normalized to TAF14 values, used as endogenous calibrator and represents the average value. Standard deviation is indicated. The average values of four sham-irradiated control mice is reported from comparison. P-values of statistical significance were calculated by Students T-test: *< 0.05 compared to control population; **< 0.01 compared to control population; # < 0.05 compared to E1 distance.

dependent modulation in individual mouse and that the effect for CACNG1 vanishes at E4 distance for the low dose (Predicted Adsorbed Dose (PAD) = 0.00021 Gy), while for TNFSF18 the threshold could be much higher (E3 distance at 1 Gy, PAD = 0.044 Gy).

3.3. Cell damage at different distances from the beam target

In order to correlate the observed gene modulations with cell damage, we used FT-IR spectroscopy analysis of lipid alteration (see Materials and Methods). In particular, the ratios between the integrated areas of different vibrational bands were calculated on a control sham-irradiated mouse and at E1, E2, E3, and E4 distance on a mouse 6 h after irradiation. Both low dose (0.1 Gy) and high dose (1 Gy) were analyzed.

The effect of radiation on the lipid content in the cell was investigated calculating the lipid/protein ratio from the amide II band centered at 1650 cm^{-1} and the total lipid stretching bands (Cakmak et al., 2012). The ratio was normalized for the same value in position E4 to take into account the variability between animals (Fig. 4a). To evaluate the alterations in tissue lipids, change in the length of the phospholipids hydrocarbon chain has been evaluated and correlated to the membrane integrity (LeVine & Wetzel, 1998). The ratio of the methylene CH_2 asymmetric band (2924 cm^{-1}) and the methyl CH_3 (2959 cm^{-1}) asymmetric band (Fig. 4b) was also evaluated to estimate the branching of the hydrocarbon chains which in turn is an indicator of membrane damage. Finally, the carbonyl content in the lipids was calculated considering the ratio of the area under the carbonyl ester band centered at 1750 cm^{-1} with the total integrated area under the lipid stretching bands (Fig. 4c). The methyl group asymmetric stretching band centered at 2959 cm^{-1} was divided by the total lipid stretching bands to give an estimation of methylation in the lipids (Figure 4(a,b,c,d).

Following these observations, the lipid/protein ratio was constant for the low dose at all distances, and comparable with the control sample, and significantly decreased for the E1 and E2 positions at high dose. A similar decrease was observed in skin of mice irradiated with 1 Gy of neutrons (Cestelli Guidi et al., 2012). The ratio between the CH_3 and CH_2 asymmetric band is also constant except for the high dose at position E1 and E2, indicating a decrease in the phospholipids chain length close to the beam target. At the same time, an increase of the unsaturation level in lipids and of the lipid methylation was observed from the olefinic and carbonyl bands.

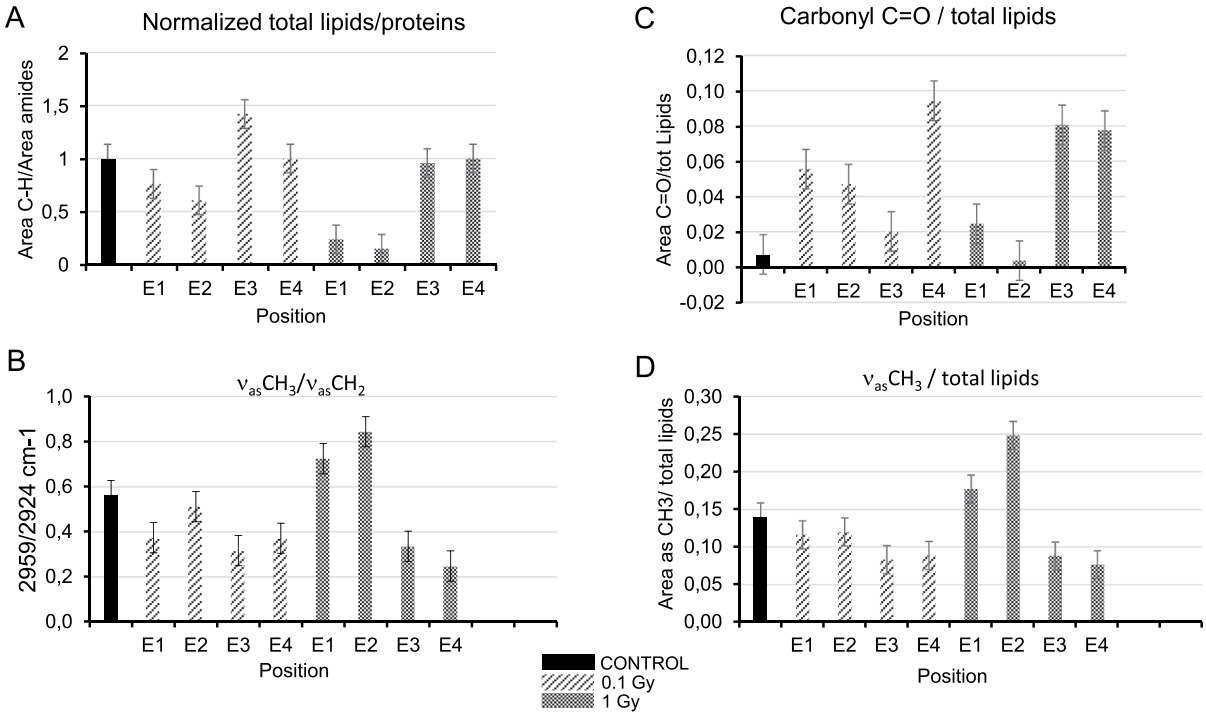

Figure 4. Quantitative analysis of the FTIR absorption bands mainly related to lipid peroxidation: (a) Area of the lipid stretching band (2800-3000 cm-1) normalized by the area of the protein amide II band (1650 cm-1); (b) area of the CH3 asymmetric peak (2959 cm-1) divided by the area under the CH2 asymmetric peak (2924 cm-1); (c) area of the carbonyl ester absorption peak divided by the total area of the lipid stretching bands; (d) area of the CH3 asymmetric band normalized by the area under the total lipid stretching bands.

This observation rules out lipid peroxidation and extensive tissue damage by proton irradiation at the lower dose at all the distances. On the other end, at 1 Gy dose a striking difference from the control is evident both at the beam target and at E2 distance. We can conclude that tissue damage is dose-dependent and it is not detectable by FTIR at the lower dose and at distance ≥ 26 mm from the beam target at the higher dose where damage could be limited to sparse cells.

4. Discussion

In this study we analyzed the transcriptional response of mice skin to 1 Gy dose of proton irradiation. As we previously showed in the case of a biologically comparable dose of neutrons, the transcriptomic changes are very different from those observed on epithelial cell lines irradiated in culture (Bufalieri et al., 2012; Chiani et al., 2009; Giusti et al., 2014; Lanza et al., 2005). As in the case of neutron irradiation, in proton-irradiated mouse skin the typical transcriptional response pathways that are activated by irradiation in proliferating cell lines are not consistently modulated. On the other hand, in analogy with the neutron irradiation, the list of significant modulations is enriched in genes involved in the immune response and in different aspects of carbon metabolism. Moreover, several gene coding for keratins or keratin-associated proteins, which appeared down-regulated by 1 Gy neutron irradiation, are also repressed by protons (even though not in a statistically significant way). We also observed a striking down-regulation of calcium signaling and up-regulation of genes involved in the control of apoptotic response as TNFSNF18, BBC3 and SNS2. The role of ion channels in radiation-induced cell death is well established (Huber et al., 2015). Modulation of ion channels such as Ca^{2+}-activated K^{+} channels or Ca^{2+}-permeable nonselective cation channels belonging to the super-family of transient receptor potential channels may contribute to radiogenic cell death as well as to DNA repair, glucose fueling, radiogenic hypermigration or lowering of the oxidative stress burden (Huber et al., 2015). TNFSF18 codes for a regulatory ligand of TNFSFR18, glucocorticoid-induced tumor necrosis factor receptor (GITR), which belongs to the tumor necrosis factor receptor superfamily. This receptor, expressed in T lymphocytes, exerts an anti-apoptotic function in these cells. It was previously reported (Wang et al., 2005) that GITR is also highly expressed in mouse skin, specifically in keratinocytes, and that it is under negative transcriptional control of p21Cip1/WAF1, independently from the cell cycle. GITR, which we found induced in neutron-irradiated skin (Fratini et al., 2011), protects keratinocytes from UVB-induced apoptosis both *in vitro* and *in vivo* (Wang et al., 2005). Its ligand coded by TNFSF18 could be involved in this protection from DNA damage-induced apoptosis as supported by its radioprotective role in murine mesothelioma cancer stem cells (Wu et al., 2018). BBC3 and SNS2 were found in a group of 29 genes differentially expressed in reconstituted human skin tissue following different doses of low-LET irradiation (Tilton et al., 2016). Once characterized the skin transcriptional response to proton irradiation, a crucial aspect to elucidate is how localized the observed modulations are. To approach this issue, we focused on two modulated genes, one induced (TNFSF18) and one repressed (CACNG1). We tested the expression of these genes in individual mice as a function of the distance from the irradiation beam target at different times and doses. Our analysis shows a clear distance-dependent trend, which is sharper for the lower dose and persisting on time for both doses. TNFSF18 is apparently still modulated at 15 mm from the target at both doses, 1 Gy and 0.1 Gy (estimated doses: 0.38 and 0.038 Gy, respectively, which are 2.6-fold, lower than the delivered dose). CACNG1 appears still modulated at 40 mm from the target at the highest dose (estimated dose: 0.0021 Gy which is 476-fold lower than the dose on target) and at 26 mm at lower dose (22.7 fold lower than the delivered dose).

5. Conclusion

Taken together, these results suggest that the diffusion distance of the gene modulation depends partially on the dose administered as well as on the particular modulated gene. For both biomarker genes the transcriptional modulation effect can propagate beyond the limit of cell damage detection, suggesting that non-hit cells may adopt a regulation similar to that one observed in hit cells. The most plausible scenario is depicted in Figure 5: Regulatory molecules (i.e. proteins or noncoding RNAs) (Nikjoo & Khvostunov, 2003; Xu et al., 2014) diffuse from hit cells (whose number strictly depends from the adsorbed dose) and transmit the transcriptional modulation to distant portions of the skin containing a much lower number of hit cells at the irradiation target and in the distant sections. This capacity of diffusing makes the modulation gradient much shallower in function of the number of the hit cells so that transcriptional modulation can be detected in considerably distant tissue portions, which adsorbed an extremely low dose of radiation. This concept which was largely accepted for electromagnetic radiation seems now extendable to particle radiation.

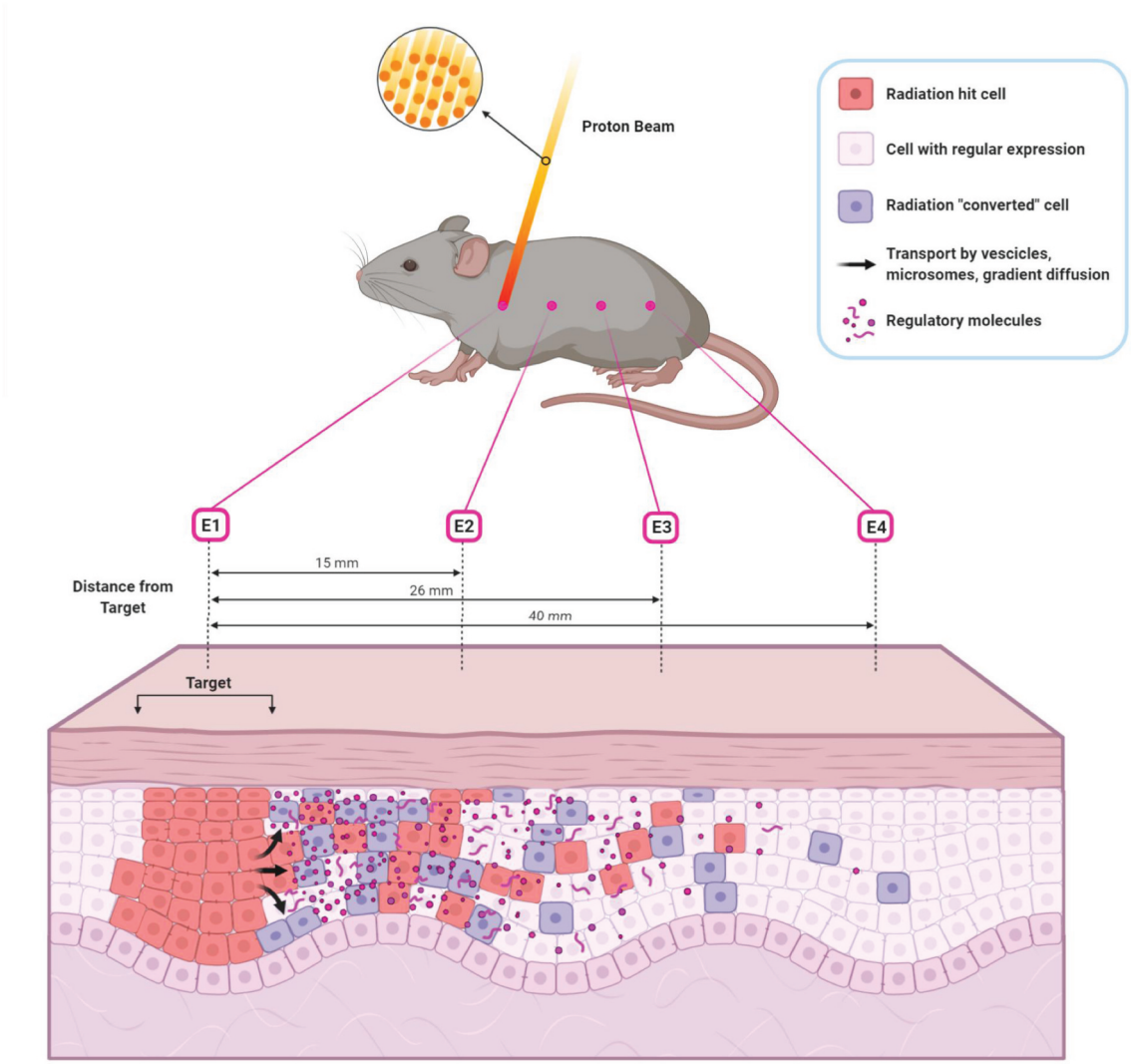

Figure 5. Model for the diffusion of transcriptional modulations: radiation-hit cells (red), distributed as predicted by Montecarlo simulation, are secreting regulatory molecules (transcription factors or regulatory RNAs, dots and sticks) which transfer the modulation to non-hit cells ("converted", gray). Created using BioRender.

Aknowledgements

This work was supported by the European Community Horizon 2020 research and innovation program under the grant agreement N. 730872, CALIPSOPlus project; by the National Institute of Nuclear Physics (INFN) under the grant agreement "Monitoring the Stress Hormone Response of Biological Tissues in Space Environment: Combined Heavy Charged Particles Irradiation and Infrared FTIR Imaging Approach", between INFN and the Academy of Scientific Research and Technology in Egypt (ASRT); by the INFN-funded project ETHICS (pre-clinical Experimental and THeoretical studies to Improve treatment and protection by Charged particleS).

Disclosure statement

No potential conflict of interest was reported by the author(s).

ORCID

Valerio Licursi http://orcid.org/0000-0002-8172-1437
Wei Wang http://orcid.org/0000-0002-1135-8265
Elena Di Nisio http://orcid.org/0000-0001-7295-3941
Francesco P. Cammarata http://orcid.org/0000-0002-0554-6649
Rosaria Acquaviva http://orcid.org/0000-0002-3139-1177
Giorgio Russo http://orcid.org/0000-0003-1493-1087
Lorenzo Manti http://orcid.org/0000-0003-0168-5040
Mariangela Cestelli Guidi http://orcid.org/0000-0002-6884-3915
Emiliano Fratini http://orcid.org/0000-0003-2522-1718
Gihan Kamel http://orcid.org/0000-0003-0854-1920
Roberto Amendola http://orcid.org/0000-0002-7019-7019
Pietro Pisciotta http://orcid.org/0000-0002-5076-9796
Rodolfo Negri http://orcid.org/0000-0002-4806-7090

References

Abdelrazzak, A. B., & El-Bahy, G. S. (2018). FT-IR spectroscopic investigation of ionizing radiation-induced damage in the small intestine of whole-body irradiated rats. *Vibrational Spectroscopy*, *99*, 146–150. https://doi.org/10.1016/j.vibspec.2018.09.007

Allison, J., Amako, K., Apostolakis, J., Araujo, H., Arce Dubois, P., Asai, M., Barrand, G., Capra, R., Chauvie, S.,

Chytracek, R., Cirrone, G. A. P., Cooperman, G., Cosmo, G., Cuttone, G., Daquino, G. G., Donszelmann, M., Dressel, M., Folger, G., Foppiano, F., Generowicz, J., & Yoshida, H. (2006). Geant4 developments and applications. *IEEE Transactions on Nuclear Science*, *53*, 270–278. https://doi.org/10.1109/TNS.2006.869826

Alsner, J., Rødningen, O. K., & Overgaard, J. (2007). Differential gene expression before and after ionizing radiation of subcutaneous fibroblasts identifies breast cancer patients resistant to radiation-induced fibrosis. *Radiotherapy and Oncology*, *83*, 261–266. https://doi.org/10.1016/j.radonc.2007.05.001

Amundson, S. A. (2008). Functional genomics in radiation biology: A gateway to cellular systems-level studies. *Radiation and Environmental Biophysics*, *47*, 25–31. https://doi.org/10.1007/s00411-007-0140-1

Boyd-Kimball, D., Castegna, A., Sultana, R., Poon, H. F., Petroze, R., Lynn, B. C., Klein, J. B., & Butterfield, D. A. (2005). Proteomic identification of proteins oxidized by Aβ(1–42) in synaptosomes: Implications for Alzheimer's disease. *Brain Research*, *1044*, 206–215. https://doi.org/10.1016/j.brainres.2005.02.086

Bray, N. L., Pimentel, H., Melsted, P., & Pachter, L. (2016). Near-optimal probabilistic RNA-seq quantification. *Nature Biotechnology*, *34*, 525–527. https://doi.org/10.1038/nbt.3519

Brooks, A. L., Retherford, J. C., & McClellan, R. O. (1974). Effect of 239 PuO 2 Particle Number and Size on the Frequency and Distribution of Chromosome Aberrations in the Liver of the Chinese Hamster. *Radiation Research*, *59*, 693. https://doi.org/10.2307/3574086

Bufalieri, F., Licursi, V., D'Antonio, M., Castrignanò, T., Amendola, R., & Negri, R. (2012). The transcriptional response of mammalian cancer cells to irradiation is dominated by a cell cycle signature which is strongly attenuated in non-cancer cells and tissues. *International Journal of Radiation Biology*, *88*, 822–829. https://doi.org/10.3109/09553002.2012.676230

Cakmak, G., Miller, L. M., Zorlu, F., & Severcan, F. (2012). Amifostine, a radioprotectant agent, protects rat brain tissue lipids against ionizing radiation induced damage: An FTIR microspectroscopic imaging study. *Archives of Biochemistry and Biophysics*, *520*, 67–73. https://doi.org/10.1016/j.abb.2012.02.012

Cestelli Guidi, M., Mirri, C., Fratini, E., Licursi, V., Negri, R., Marcelli, A., & Amendola, R. (2012). In vivo skin leptin modulation after 14 MeV neutron irradiation: A molecular and FT-IR spectroscopic study. *Analytical and Bioanalytical Chemistry*, *404*, 1317–1326. https://doi.org/10.1007/s00216-012-6018-3

Cestelli Guidi, M., Piccinini, M., Marcelli, A., Nucara, A., Calvani, P., & Burattini, E. (2005). Optical performances of SINBAD. *The Synchrotron INfrared Beamline at DA?NE*, *22*, 2810–2817.

Chiani, F., Iannone, C., Negri, R., Paoletti, D., D'Antonio, M., De Meo, P. D., & Castrignanò, T. (2009). Radiation Genes: A database devoted to microarrays screenings revealing transcriptome alterations induced by ionizing radiation in mammalian cells. *Database*, *2009*. https://doi.org/doi:10.1093/database/bap007

Cohen, L., & Awschalom, M. (1982). Fast Neutron Radiation Therapy. *Annual Review of Biophysics and Bioengineering*, *11*, 359–390. https://doi.org/10.1146/annurev.bb.11.060182.002043

Crow, M., Lim, N., Ballouz, S., Pavlidis, P., & Gillis, J. (2019). Predictability of human differential gene expression. *Proceedings of the National Academy of Sciences*, *116*, 6491–6500. https://doi.org/10.1073/pnas.1802973116

Dennis, G., Sherman, B. T., Hosack, D. A., Yang, J., Gao, W., Lane, H. C., & Lempicki, R. A. (2003). DAVID: Database for Annotation, Visualization, and Integrated Discovery. *Genome Biology*, *4*, R60. https://doi.org/10.1186/gb-2003-4-9-r60

Durante, M. (2014). New challenges in high-energy particle radiobiology. *The British Journal of Radiology*, *87*, 20130626. https://doi.org/10.1259/bjr.20130626

Durante, M., & Flanz, J. (2019). Charged particle beams to cure cancer: Strengths and challenges. *Seminars in Oncology*, *46*, 219–225. https://doi.org/10.1053/j.seminoncol.2019.07.007

Fratini, E., Licursi, V., Artibani, M., Kobos, K., Colautti, P., Negri, R., Amendola, R., & Ryffel, B. (2011). Dose-dependent onset of regenerative program in neutron irradiated mouse skin. Ryffel B *Editor*. *PLoS ONE*, *6*, e19242. https://doi.org/10.1371/journal.pone.0019242

Gentleman, R. C., Carey, V. J., Bates, D. M., Bolstad, B., Dettling, M., Dudoit, S., Ellis, B., Gautier, L., Ge, Y., Gentry, J., Hornik, K., Hothorn, T., Huber, W., Iacus, S., Irizarry, R., Leisch, F., Li, C., Maechler, M., Rossini, A. J., Sawitzki, G., & Zhang, J. (2004). Bioconductor: Open software development for computational biology and bioinformatics. *Genome Biology*, *5*, R80. https://doi.org/10.1186/gb-2004-5-10-r80

Gianoncelli, A., Vaccari, L., Kourousias, G., Cassese, D., Bedolla, D. E., Kenig, S., Storici, P., Lazzarino, M., & Kiskinova, M. (2015). Soft X-ray microscopy radiation damage on fixed cells investigated with synchrotron radiation FTIR microscopy. *Scientific Reports*, *5*, 10250. https://doi.org/10.1038/srep10250

Girdhani, S., Lamont, C., Hahnfeldt, P., Abdollahi, A., & Hlatky, L. (2012). Proton irradiation suppresses angiogenic genes and impairs cell invasion and tumor growth. *Radiation Research*, *178*, 33–45. https://doi.org/10.1667/RR2724.1

Giusti, N., Bufalieri, F., Licursi, V., Castrignanò, T., D'Antonio, M., Amendola, R., & Negri, R. (2014). General features of the transcriptional response of mammalian cells to low- and high-LET irradiation. *Rendiconti Lincei*, *25*, (S1):69–74. https://doi.org/10.1007/s12210-013-0274-9

Givehchi, N., Marchetto, F., Valastro, L. M., Ansarinejad, A., Attili, A., Garella, M. A., Giordanengo, S., Monaco, V., Montero, J. P., Sacchi, R., Boriano, A., Bourhaleb, F., Cirio, R., La Rosa, A., Pecka, A., Peroni, C., Cirrone, G. A. P., Cuttone, G., Donetti, M., Iliescu, S., & Raffaele, L. (2011). Online beam monitoring in the treatment of ocular pathologies at the INFN Laboratori Nazionali del Sud-Catania. *Physica Medica*, *27*, 233–240. https://doi.org/10.1016/j.ejmp.2010.10.004

Hall, D. C., Makarova, A., Paganetti, H., & Gottschalk, B. (2016). Validation of nuclear models in Geant4 using the dose distribution of a 177 MeV proton pencil beam. *Physics in Medicine and Biology*, *61*, N1–N10. https://doi.org/10.1088/0031-9155/61/1/N1

Hamada, N., Bouffler, S., & Woloschak, G. E. (2016). Special issue: Tissue reactions to ionizing radiation exposure. *Mutation Research/Reviews in Mutation Research*, *770*, 217–218. https://doi.org/10.1016/j.mrrev.2016.06.002

Huang, D. W., Sherman, B. T., & Lempicki, R. A. (2009). Systematic and integrative analysis of large gene lists using DAVID bioinformatics resources. *Nature Protocols*, *4*, 44–57. https://doi.org/10.1038/nprot.2008.211

Huber, S. M., Butz, L., Stegen, B., Klumpp, L., Klumpp, D., & Eckert, F. (2015). Role of ion channels in ionizing radiation-induced cell death. *Biochimica Et Biophysica Acta (BBA) - Biomembranes*, *1848*, 2657–2664. https://doi.org/10.1016/j.bbamem.2014.11.004

Kamel, G., Lefrançois, S., Al-Najdawi, M., Abu-Hanieh, T., Saleh, I., Momani, Y., & Dumas, P. (2017). EMIRA: The infrared synchrotron radiation beamline at SESAME. *Synchrotron Radiation News*, *30*, 8–10. https://doi.org/10.1080/08940886.2017.1338415

Lanza, V., Pretazzoli, V., Olivieri, G., Pascarella, G., Panconesi, A., & Negri, R. (2005). Transcriptional Response of Human Umbilical Vein Endothelial Cells to Low Doses of Ionizing Radiation. *Journal of Radiation Research*, *46*, 265–276. https://doi.org/10.1269/jrr.46.265

LeVine, S. M., & Wetzel, D. L. (1998). Chemical analysis of multiple sclerosis lesions by FT-IR microspectroscopy. *Free Radical Biology and Medicine*, *25*, 33–41. https://doi.org/10.1016/S0891-5849(98)00019-7

Licursi, V., Cestelli Guidi, M., Del Vecchio, G., Mannironi, C., Presutti, C., Amendola, R., & Negri, R. (2017). Leptin induction following irradiation is a conserved feature in mammalian epithelial cells and tissues. *International Journal of Radiation Biology*, *93*, 947–957. https://doi.org/10.1080/09553002.2017.1339918

Love, M. I., Huber, W., & Anders, S. (2014). Moderated estimation of fold change and dispersion for RNA-seq data with DESeq2. *Genome Biology*, *15*, 550. https://doi.org/10.1186/s13059-014-0550-8

Marín, A., Martín, M., Liñán, O., Alvarenga, F., López, M., Fernández, L., Büchser, D., & Cerezo, L. (2015). Bystander effects and radiotherapy. *Reports of Practical Oncology & Radiotherapy*, *20*, 12–21. https://doi.org/10.1016/j.rpor.2014.08.004

Miralbell, R., Lomax, A., Cella, L., & Schneider, U. (2002). Potential reduction of the incidence of radiation-induced second cancers by using proton beams in the treatment of pediatric tumors. *International Journal of Radiation Oncology*Biology*Physics*, *54*, 824–829. https://doi.org/10.1016/S0360-3016(02)02982-6

Mole, R. H. (1953). Whole Body Irradiation—Radiobiology or Medicine? *The British Journal of Radiology*, *26*, 234–241. https://doi.org/10.1259/0007-1285-26-305-234

Mothersill, C., & Seymour, C. B. (2006). Radiation-induced bystander effects and the DNA paradigm: An "out of field" perspective. *Mutation Research/Fundamental and Molecular Mechanisms of Mutagenesis*, *597*, 5–10. https://doi.org/10.1016/j.mrfmmm.2005.10.011

Nielsen, S., Bassler, N., Grzanka, L., Swakon, J., Olko, P., Andreassen, C. N., Overgaard, J., Alsner, J., & Sørensen, B. S. (2017). Differential gene expression in primary fibroblasts induced by proton and cobalt-60 beam irradiation. *Acta Oncologica*, *56*, 1406–1412. https://doi.org/10.1080/0284186X.2017.1351623

Nikjoo, H., & Khvostunov, I. K. (2003). Biophysical model of the radiation-induced bystander effect. *International Journal of Radiation Biology*, *79*, 43–52. https://doi.org/10.1080/0955300021000034701

Panganiban, R. A. M., Mungunsukh, O., & Day, R. M. (2013). X-irradiation induces ER stress, apoptosis, and senescence in pulmonary artery endothelial cells. *International Journal of Radiation Biology*, *89*, 656–667. https://doi.org/10.3109/09553002.2012.711502

Pisciotta, P., Cammarata, F. P., Stefano, A., Romano, F., Marchese, V., Torrisi, F., Forte, G. I., Cella, L., Cirrone, G. A. P., Petringa, G., Gilardi, M. C., Cuttone, G., & Russo, G. (2018). Monte Carlo GEANT4-based application for in vivo RBE study using small animals at LNS-INFN preclinical hadrontherapy facility. *Physica Medica*, *54*, 173–178. https://doi.org/10.1016/j.ejmp.2018.07.003

Russo, G., Pisciotta, P., Cirrone, G. A. P., Romano, F., Cammarata, F., Marchese, V., Forte, G. I., Lamia, D., Minafra, L., Bravatá, V., Acquaviva, R., Gilardi, M. C., & Cuttone, G. (2017). Preliminary study for small animal preclinical hadrontherapy facility. *Nuclear Instruments and Methods in Physics Research Section A: Accelerators, Spectrometers, Detectors and Associated Equipment*, *846*, 126–134. https://doi.org/10.1016/j.nima.2016.10.021

Santivasi, W. L., & Xia, F. (2014). Ionizing radiation-induced dna damage, response, and repair. *Antioxidants & Redox Signaling*, *21*, 251–259. https://doi.org/10.1089/ars.2013.5668

Tian, J., Zhao, W., Tian, S., Slater, J. M., Deng, Z., & Gridley, D. S. (2011). Expression of genes involved in mouse lung cell differentiation/regulation after acute exposure to photons and protons with or without low-dose preirradiation. *Radiation Research*, *176*, 553–564. https://doi.org/10.1667/RR2601.1

Tilton, S. C., Markillie, L. M., Hays, S., Taylor, R. C., & Stenoien, D. L. (2016). Identification of differential gene expression patterns after acute exposure to high and low doses of low-let ionizing radiation in a reconstituted human skin tissue. *Radiation Research*, *186*, 531–538. https://doi.org/10.1667/RR14471.1

Tommasino, F., & Durante, M. (2015). Proton radiobiology. *Cancers*, *7*, 353–381. https://doi.org/10.3390/cancers7010353

Vitti, E. T., & Parsons, J. L. (2019). The radiobiological effects of proton beam therapy: Impact on DNA damage and repair. *Cancers*, *11*, 946. https://doi.org/10.3390/cancers11070946

Wang, J., Devgan, V., Corrado, M., Prabhu, N. S., El-Deiry, W. S., Riccardi, C., Pandolfi, P. P., Missero, C., & Dotto, G. P. (2005). Glucocorticoid-induced tumor necrosis factor receptor is a p21 <sup>transcriptional target conferring resistance of Keratinocytes to UV light-induced apoptosis. *Journal of Biological Chemistry*, *280*, 37725–37731. https://doi.org/10.1074/jbc.M507976200

Weichselbaum, R. R., Hallahan, D. E., Sukhatme, V., Dritschilo, A., Sherman, M. L., & Kufe, D. W. (1991). Biological consequences of gene regulation after ionizing radiation exposure. *JNCI Journal of the National Cancer Institute*, *83*, 480–484. https://doi.org/10.1093/jnci/83.7.480

Westbury, C. B., & Yarnold, J. R. (2012). Radiation fibrosis — Current clinical and therapeutic perspectives. *Clinical Oncology*, *24*, 657–672.

Woloschak, G. E., & Chang-Liu, C. M. (1990). Differential modulation of specific gene expression following high- and low-LET radiations. *Radiation Research*, *124*, 183–187. https://doi.org/10.2307/3577864

Wu, L., Blum, W., Zhu, C.-Q., Yun, Z., Pecze, L., Kohno, M., Chan, M.-L., Zhao, Y., Felley-Bosco, E., Schwaller, B., & De Perrot, M. (2018). Putative cancer stem cells may be the key target to inhibit cancer cell repopulation between the intervals of chemoradiation in murine mesothelioma. *BMC Cancer*, *18*, 471. https://doi.org/10.1186/s12885-018-4354-1

Xu, S., Ding, N., Pei, H., Hu, W., Wei, W., Zhang, X., Zhou, G., & Wang, J. (2014). MiR-21 is involved in radiation-induced bystander effects. *RNA Biology*, *11*, 1161–1170. https://doi.org/10.4161/rna.34380

Xue, L., Yu, D., Furusawa, Y., Okayasu, R., Tong, J., Cao, J., & Fan, S. (2009). Regulation of ATM in DNA double strand break repair accounts for the radiosensitivity in human cells exposed to high linear energy transfer ionizing radiation. *Mutation Research/Fundamental and Molecular Mechanisms of Mutagenesis*, *670*, 15–23. https://doi.org/10.1016/j.mrfmmm.2009.06.016

Yilmaz, M. T., Elmali, A., & Yazici, G. (2019). Abscopal effect, from myth to reality: From radiation oncologists' perspective. *Cureus*, *11*, e3860. https://doi.org/10.7759/cureus.3860